



Antibacterial performance of nanoscaled visible-light responsive platinum-containing titania photocatalyst *in vitro* and *in vivo*

Yao-Hsuan Tseng^a, Der-Shan Sun^b, Wen-Shiang Wu^b, Hao Chan^c, Ming-Syuan Syue^a, Han-Chen Ho^d, Hsin-Hou Chang^{b,c,*}

^a Department of Chemical Engineering, National Taiwan University of Science and Technology, Taipei, Taiwan

^b Department of Molecular Biology and Human Genetics, Tzu-Chi University, Hualien, Taiwan

^c Graduate Institute of Medical Science, Tzu-Chi University, Hualien, Taiwan

^d Department of Anatomy, Tzu-Chi University, Hualien, Taiwan

ARTICLE INFO

Article history:

Received 15 October 2012

Received in revised form 1 February 2013

Accepted 14 March 2013

Available online 29 March 2013

Keywords:

TiO₂

Platinum-containing TiO₂

Visible light responsive photocatalyst

ABSTRACT

Background: Traditional antibacterial photocatalysts are primarily induced by ultraviolet light to elicit antibacterial reactive oxygen species. New generation visible-light responsive photocatalysts were discovered, offering greater opportunity to use photocatalysts as disinfectants in our living environment. Recently, we found that visible-light responsive platinum-containing titania (TiO₂-Pt) exerted high performance antibacterial property against soil-borne pathogens even in soil highly contaminated water. However, its physical and photocatalytic properties, and the application *in vivo* have not been well-characterized.

Methods: Transmission electron microscopy, energy dispersive spectroscopy, X-ray photoelectron spectroscopy, X-ray diffraction, ultraviolet–visible absorption spectrum and the removal rate of nitrogen oxides were therefore analyzed. The antibacterial performance under *in vitro* and *in vivo* conditions was evaluated.

Results: The apparent quantum efficiency for visible light illuminated TiO₂-Pt is relatively higher than several other titania photocatalysts. The killing effect achieved approximately 2 log reductions of pathogenic bacteria *in vitro*. Illumination of injected TiO₂-Pt successfully ameliorated the subcutaneous infection in mice.

Conclusions: This is the first demonstration of *in vivo* antibacterial use of TiO₂-Pt nanoparticles. When compared to nanoparticles of some other visible-light responsive photocatalysts, TiO₂-Pt nanoparticles induced less adverse effects such as exacerbated platelet clearance and hepatic cytotoxicity *in vivo*.

General significance: These findings suggest that the TiO₂-Pt may have potential application on the development of an antibacterial material in both *in vitro* and *in vivo* settings.

© 2013 Elsevier B.V. All rights reserved.

1. Introduction

Disinfectants and antibiotics are antimicrobial agents extensively used in various *in vitro* and *in vivo* settings. They are essential for infection control and aid in the prevention of nosocomial infections. Compared to antibiotics, which provide comparatively selective activity against microorganisms, disinfectants typically have a broader biocidal spectrum and are usually used with inanimate objects [1,2]. Traditional chemical-based disinfectants, such as alcohols, aldehydes, iodine, phenols, and chlorine, have been used for centuries in environmental cleaning. Although these disinfectants are highly efficient against pathogenic microbes, they also have problems. These disinfectants are usually volatile, and their byproducts can be toxic and carcinogenic to humans. As the widespread use of antibiotics and the emergence of

more-resistant and -virulent strains of microorganisms became great clinical challenges [3–8], the establishment and development of novel antibacterial strategies is, therefore, significant in the control of human pathogens and prevention of infectious diseases. From this point of view, photocatalyst-based antibacterial agents are conceptually feasible alternative approaches.

Classical photocatalyst generates pairs of electrons and holes (electron vacancy in valence band) upon ultraviolet light (UV) illumination. The electrons and holes induced by the reactions have strong reducing and oxidizing activities, and subsequently react with atmospheric water and oxygen (H₂O and O₂) to yield reactive oxygen species (ROS), such as hydroxyl radicals (•OH), superoxide anions (O₂⁻), and hydrogen peroxide (H₂O₂) [9]. These ROS can oxidize organic substances and exert the antibacterial function [10]. Titanium dioxide (TiO₂) is the most widely used UV-responsive photocatalyst [11], which has been demonstrated to exert antibacterial effect in various forms that includes nanoparticles, thin films and polymer-composites [12–23]. The UV-light, however, can damage eyes and skin [24]. These side effects limit the use of UV-responsive photocatalysts in our living environments. Recently,

* Corresponding author at: Room D407, Tzu-Chi University, No. 701, Section 3, Chung-Yang Road, Hualien 97004, Taiwan. Tel.: +886 3 8565301x2667; fax: +886 3 8578386.

E-mail address: hhchang@mail.tcu.edu.tw (H.-H. Chang).

photocatalysts using visible light as alternative energy source were developed [25,26], which exerted antibacterial property [22,27,28]. These visible light responsive photocatalysts may also increase the light-spectrum absorption range, because the UV range of solar irradiation reached to the Earth's surfaces is estimated to be only 2–3% [29]. At the same time, the emergence of antibiotic-resistant bacteria in public environments leads to an urgent need of alternative disinfection approaches [3–7]. Visible-light responsive photocatalysts have potential advantages for use in a variety of settings to reduce the transmission of pathogens in the public environments. Impurity doping of different materials such as anion and cation on TiO₂ is a generally used strategy to extend the absorption spectrum into the visible-light range [25–28,30]. Since silver contains antibacterial property [31], a composite with silver nanoparticles is another approach to increase both antibacterial performance and visible-light responsiveness of titania photocatalysts [14,19,32]. Iron can extend the absorption of the light to the visible region and serve as an electron or hole scavenger on the surface of TiO₂ to result in better separation of free carriers [33]. As visible-light responsive photocatalysts are currently under a developmental stage, their antibacterial property [27,28,34], however, is unable to compare with the high antibacterial performance of traditional chemical disinfectants [1]. Thus, development of a high performance photocatalyst is needed.

The antibacterial property of platinum-loaded titania (TiO₂/Pt) was firstly reported to be activated by UV-irradiation [35]. Recently, we found that platinum-containing titania (TiO₂-Pt) photocatalyst contains superior antibacterial property against soil-borne pathogens even in soil-contaminated water [36]. However, the physical and photocatalytic properties under visible light illumination and the potential antibacterial application *in vivo* have not been well-characterized. As a result, to characterize the crystal morphology, composites of Pt element, Pt valence states, crystal structure and light absorption spectrum, we employed transmission electron microscopy (TEM), energy dispersive spectroscopy (EDS), X-ray photoelectron spectroscopy (XPS), X-ray diffraction (XRD) and UV-visible absorption spectrum, respectively. The photocatalytic performance was characterized by measuring the removal rate of nitrogen oxides (NO_x). In addition, the antibacterial property of the TiO₂-Pt against nosocomial infected pathogens *Staphylococcus aureus*, and *Acinetobacter baumannii*, and exotoxin-producing *Streptococcus pyogenes* was further evaluated under visible light illumination. The data suggest that TiO₂-Pt substrates have superior visible-light induced bactericidal property against human pathogens (approximately 2 log reduction) as compared to several other commercially available and laboratory prepared photocatalysts (ST01, P-25, C200, BA-PW25, etc. [23,34,37–40]; achieved approximately 0–1 log reduction under visible light). In addition, the potential *in vivo* usage was further evaluated by nanoparticle treatments using a mouse model, in which the potential applications *in vivo* are discussed.

2. Materials and methods

2.1. Preparation and characterization of photocatalysts

Following previously described methods [36], platinum-containing nano-structured TiO₂ particles (TiO₂-Pt) were prepared by the photoreduction process using chloroplatinic acid (H₂PtCl₆) and commercial TiO₂ nanoparticles (ST01; Ishihara, Singapore) as a platinum precursor and a pristine photocatalyst, respectively. The photocatalyst crystal phase was identified using X-ray diffractometry with Cu K α radiation ($\lambda = 0.154$ nm, D/Max RC; Rigaku, Tokyo, Japan). Material compositions were determined by X-ray photoelectron spectroscopy (SSI-M probe XPS system; Perkin Elmer, Waltham, MA). A diffuse-reflectance scanning spectrophotometer (UV-2450; Shimadzu, Kyoto, Japan) was employed to obtain the UV-visible absorption spectra of the powders. The reflectance data were converted to the absorbance values, F(R),

based on the Kubelka–Munk theory. Measuring average particle size and morphology was performed by transmission electron microscopy (TEM, Philips Tecnai F20 G2 FEI-TEM). The specific surface area of the powders was measured by nitrogen adsorption using the Brunauer, Emmet, and Teller (BET) equation (Micrometrics Model ASAP 2400). The amount of Pt that was released from the TiO₂-Pt surfaces into the deionized (D.I.) water (0.1 g TiO₂-Pt powder in 100 mL H₂O, pH 7.4) was measured by inductively coupled plasma atomic emission spectrometry (ICP-AES, JY 2000-2, Horiba).

2.2. Photocatalytic activity for NO oxidation

The NO_x degradation was carried out at room temperature using an air stream containing 1.0 ppm NO as feedstock. The reaction system and procedure were described in detail in our previous papers [39,41–43]. The fundamental photocatalytic activity of prepared Pt/TiO₂ was evaluated by the de-NO_x photocatalytic activity implemented in relation to ISO22197-1 [44].

2.3. Bacterial strains and culture

Bacteria *S. pyogenes* (strain M29588), *S. aureus* (strain SA02) (without antibiotic resistance), and pan-drug resistance *A. baumannii* (PDRAB; strain M36788), are clinical isolates from the Buddhist Tzu-Chi General Hospital, Hualien, Taiwan. *S. pyogenes* and *S. aureus* were grown in tryptic soy broth supplemented with 0.5% yeast extract (TSBY) broth or TSBY broth agar (MDBio, Inc. Taipei, Taiwan) [27]. *A. baumannii* were maintained and grown in Luria–Bertani broth (LB) or LB agar (MDBio, Inc. Taipei, Taiwan) [27].

2.4. Photocatalytic reaction and detection of viable bacteria

The elimination of bacteria by photocatalysis was determined using previously described methods [27,28]. Bacteria and TiO₂-Pt loaded 24-well plates (1×10^5 CFU + saline-rinsed TiO₂-Pt nanoparticles 50 μ g/ml) were placed under an incandescent lamp (ClassicTone incandescent lamp, 60 W; Philips) for photocatalytic reaction. The illuminations were initially carried out with illumination density of 48 mW/cm² for 75 min (337.5 J/cm²). In dose-dependence experiments, illuminations were performed with illumination density of 28, 34 and 48 mW/cm² for 30 min (1×10^3 , 3×10^3 , 1×10^4 lx; and 50.4, 61.2 and 86.4 J/cm², respectively). In the kinetic analysis, illuminations were conducted with illumination density of 48 mW/cm² for 10, 15, 30, 45 and 75 min (28.8, 43.2, 86.4, 129.6 and 337.5 J/cm²). The reaction temperature was 15 °C. After illumination, the surviving bacteria were quantified using the standard plating method. Commercially available UV-responsive photocatalysts ST01 [39], UV100 (Sachtleben, Germany) [34], Degussa P-25 (Evonik Degussa, Essen, Germany) [40] and UV/Vis-responsive photocatalyst BA-PW25 (Ecodevice, Tokyo, Japan) [37] were used as comparisions.

2.5. Transmission electron microscopy (TEM), scanning electron microscopy (SEM) and energy dispersive X-ray spectroscopy (EDS) analyses

The bacterial samples were negatively stained and then analyzed by TEM using a Hitachi H-7500 transmission electron microscope. The SEM and EDS were analyzed using a JEM-3010 scanning electron microscope (JEOL, Japan) equipped with energy dispersive X-ray spectrometer following previously described methods (SEM [34,45], EDS [45]).

2.6. Air-pouch infection mouse model

Animal care and the air pouch infection were performed as described [36,45,46]. Anesthetic C57Bl/6J mice were subcutaneously injected with 1 ml air to form an air pouch. Suspensions of the *S. aureus* (log phase,

3×10^5 CFU, 0.2 ml phosphate buffered saline [PBS]) and the photocatalysts (D.I. H₂O rinsed twice; 500 µg/mL, 0.3 mL PBS) were injected into the air pouch sequentially. Bacteria–photocatalyst mixtures in the air pouches were then illuminated by skin-penetrative visible light using a cold-light source (KL-1500 LCD, Carl Zeiss; visible light, 60 mW/cm², 30 min), by which the mouse skin will not be damaged by heat during illumination. The number of surviving bacteria (CFU) was determined using the standard plating method. The research methods applied regarding the experimental mice were approved by the Institutional Animal Care and Use Committee of Tzu Chi University (approval ID: 95012).

2.7. Statistical analysis

All results were calculated from data at least of three independent experiments. T-test was used to assess statistical significance of differences in results of the antimicrobial effects. A *P* value of less than 0.05 (*P* < 0.05) was considered significant. The statistical tests were carried out and output to graphs using the Microsoft Excel (Microsoft Taiwan, Taipei, Taiwan) and SigmaPlot (Systat Software, Point Richmond, CA) software.

2.8. Supplemental methods

More detailed descriptions referring to the materials and methods used in this study could be obtained from the supplemental materials online.

3. Results

3.1. Characterizations of TiO₂-Pt

Transmission electron microscopy (TEM) images showed the morphology of the Pt-deposited titanium oxide (Fig. 1A-1 and 2). The deposited Pt particles measuring approximately 2–3 nm were dispersed on the surface of the pristine photocatalyst ST01 (Ishihara) [39], and the mean particle size of ST01 is near 8 nm. Parallel results of energy dispersive spectroscopy (EDS) (Fig. 1A-3) further indicated that the small gray particles in Fig. 1A-1 and 2 are deposited with platinum (Fig. 1A-1 and 2 arrow indicated spots).

To investigate the Pt states on the prepared TiO₂, the Pt 4f levels were measured by X-ray photoelectron spectroscopy (XPS) (Fig. 1B). Literatures have reported that the incorporation of noble metal in/on the TiO₂ results in formation of Ti³⁺ chemical state, peak at 457.9 eV. This phenomenon is primarily observed in the presence of plenty amount of doping metal, for example, M/Ti = 3–10 mol% [47–49]. The peak associated with the Ti³⁺ species was not found for TiO₂-Pt because of low Pt content (0.5 mol%; suppl. Fig. S1). Binding energy of three different valence states, Pt⁰, Pt^{II} and Pt^{IV}, was observed at 74.9, 76.2 and 77.3 eV, respectively [50]. The atomic ratio of Pt⁰, Pt^{II} and Pt^{IV} on Pt 4f_{5/2} was computed as 44%, 31%, and 25%, respectively. During the photodeposition of platinum, the distribution of valence state (*i.e.*, metallic, metal oxide) changes with pH. The metal oxide content gradually increases as the reaction solution pH increases [50]. Therefore, the Pt⁰ fraction is higher than other oxide states due to its slightly acidic condition. The specific surface area of ST01 and TiO₂-Pt measured by nitrogen adsorption were 185.3 and 182.1 m²/g,

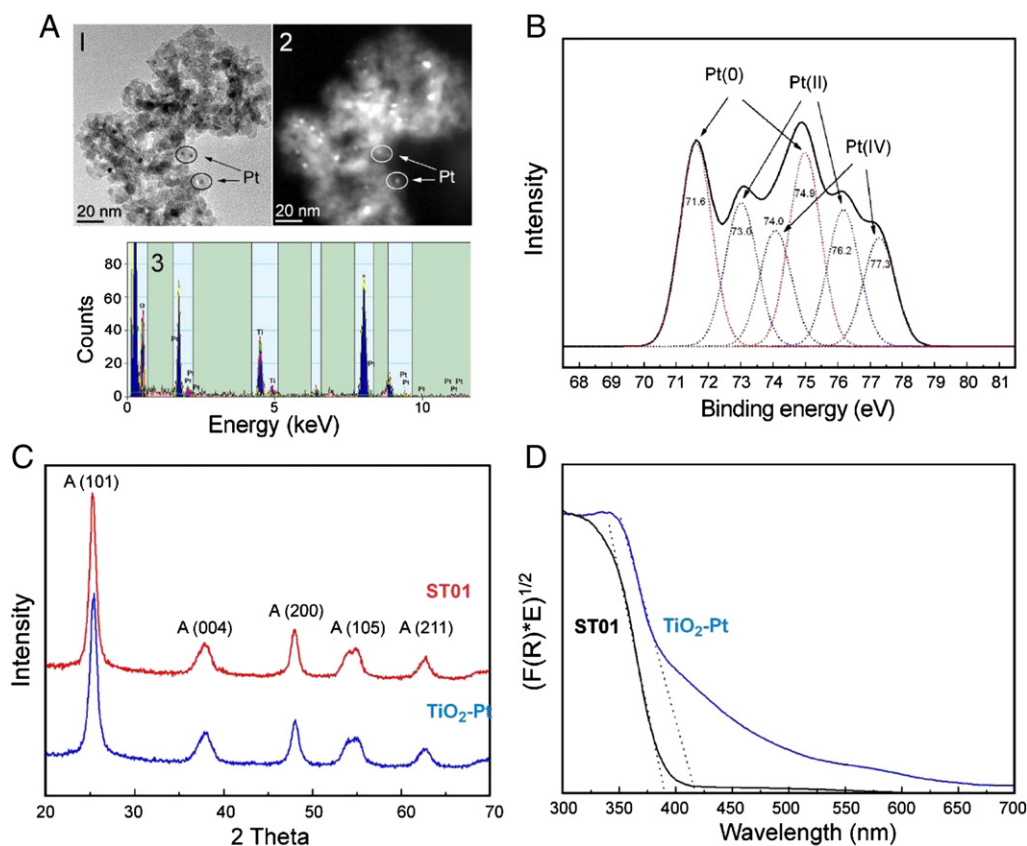


Fig. 1. Transmission electron microscopy (TEM) images and spectrum analyses of TiO₂-Pt. The representative images were captured in bright field (A-1) and dark field (A-2), respectively. Through energy dispersive spectroscopy (EDS) analysis (A-3), Pt was found in the arrows pointed spots (A-1, 2). Scale bar: 20 nm. Deconvolution of Pt 4f XPS spectra for TiO₂-Pt (B), and XRD pattern (C) and UV-visible absorption spectra (D) of TiO₂-Pt and ST01 were indicated.

respectively. The results indicate that the addition of Pt produced insignificant changes in the specific surface area of TiO₂ particle size due to low Pt content and low calcination temperature in this preparation procedure. Furthermore, TEM observation confirmed that the prepared TiO₂ powders had an almost spherical and nonporous form. Therefore, this relationship can be expressed by a simple equation, assuming a spherical and nonporous particle: $d_{\text{BET}} = 6000 / \rho A$, where d_{BET} is the calculated particle size (nm), ρ the density of TiO₂ (3.84 g/cm³), and A is the specific surface area (m²/g) [51]. Thus, the d_{BET} of TiO₂-Pt sample is around 8.6 nm by the above equation. The X-ray diffraction (XRD) patterns of TiO₂ samples were also examined (Fig. 1C). The peaks indicated as (101), (004), (200), (105), and (211) in Fig. 1C, revealed the reflection characteristics of TiO₂ anatase phase appearing in all samples (Fig. 1C). The rutile phase does not appear due to the low-temperature calcination. The crystallite sizes of the prepared photocatalysts are determined from a half width of (101) peak ($2\theta = 25.4^\circ$) using the Scherrer formula [52]. Accordingly, the anatase grain size of TiO₂-Pt and ST01 were around 9–7 nm, which is consistent with the observations of TEM images (Fig. 1A) and the estimated result from specific surface area. No peaks corresponding to crystalline phase of Pt metal and PtO_x ($2\theta = 39.8^\circ, 46.2^\circ, 67.5^\circ$) were found due to small crystallite size and low Pt content. The results indicate that the addition of Pt salt produced insignificant changes in the primary TiO₂ particle size.

To investigate the light absorption property, UV–visible diffuse reflectance spectra of TiO₂-Pt and ST01 samples were analyzed (Fig. 1D). This reflectance data was converted by the instrument software to absorbance values, $F(R)$, based on the Kubelka–Munk theory. TiO₂-Pt exhibited a good visible-light absorption tail up to over 700 nm, and a sharp edge that extended to ~432 nm corresponding to a band gap of ~2.87 eV was observed (Fig. 1D). Therefore, the platinum species on the sample may play a role as the sensitizer for visible-light absorption.

3.2. Photocatalytic degradation of NO over TiO₂-Pt under visible light illumination

Nitrogen oxides (NO_x) are air pollutants [53]. Oxidation of NO was used to determine photocatalytic reactivity in various TiO₂ photocatalytic applications [50,54–56]. Before the antibacterial test, the reaction of photocatalytic oxidation of NO was used to evaluate the visible-light-responsive activity and estimate the apparent quantum efficiency of TiO₂ samples. The electron–hole pair ($e^- - h^+$) generated upon light excitation is trapped at the TiO₂ surfaces as spatially separated redox active sites. Some studies report the formation of reactive oxygen species, such as superoxide ion ($O_2^{\bullet-}$), atomic oxygen (O), O^- , OH and HO₂ radicals on the surface of TiO₂ irradiated with UV light [11]. The general mechanism of NO_x oxidation by photocatalyst is as follows. Hydrogen ions and hydroxide ions are dissociated from water. The active oxygen species are produced on the TiO₂ surfaces. The nitric monoxide is oxidized to nitric acid or nitrous acid by active oxygen species. Based on the gas-phase chemistry of NO_x [54], NO is converted to HNO₃ as a consecutive photooxidation via a NO₂ intermediate.



Photocatalytic TiO₂-Pt mediated removal of NO and NO_x was compared with the pristine photocatalyst ST01, two UV-responsive photocatalysts UV100, P-25, and two visible-light responsive photocatalysts BA-PW25 (commercially available) [37] and C200 (a carbon-containing TiO₂) [23] (Fig. 2A). The activity levels of these photocatalysts fell in the order of TiO₂-

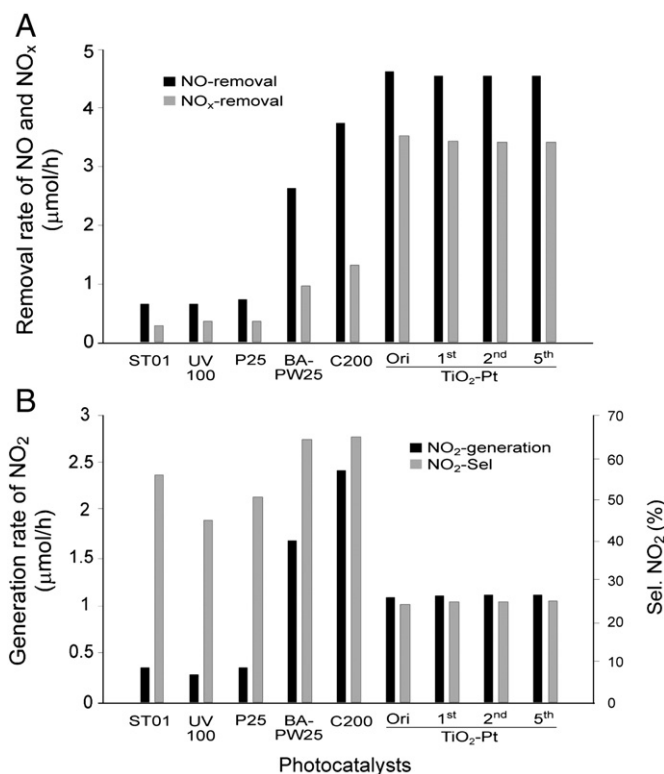


Fig. 2. Average removal rate of NO and NO_x, and generation rate of NO₂ on various photocatalysts under visible-light irradiation. Removal rate of NO and NO_x (A) and generation rate of NO₂ were indicated (μmol/h) (B). Catalyst loading: 0.1 g, irradiation intensity: 1 mW/cm², inlet concentration of NO: 1 ppm, inlet flow rate: 1 L/min, reaction temperature: 26 °C. TiO₂-Pt/Ori groups: original/as-prepared material without reuses. TiO₂-Pt/1st, 2nd, 5th groups: TiO₂-Pt samples that were used for the 1st, 2nd and 5th reuse cycles.

Pt > C200 > BA-PW25 ≫ ST01 ~ UV100 ~ P25 under visible light (blue LED). The pure TiO₂ samples (ST01, UV100, and P25) have little photoactivities due to their large bandgap. The generation of NO₂ and selectivity of NO₂ ($\text{Sel. NO}_2 = [\text{NO}_2]_{\text{generated}} / [\text{NO}]_{\text{converted}}$) of the photocatalyst have a great effect on the NO_x-removal activity, as shown in Fig. 2B. For example, the TiO₂-Pt has 3.6 times the NO_x removal activity of BA-PW25 even if the TiO₂-Pt has only 1.7 times the NO removal activity of BA-PW25. It might be that the Pt particle has a good affinity to NO₂. This is valuable for photocatalytic removal of NO, because NO₂ is an undesired intermediate in the consecutive oxidation of NO; the threshold concentrations of NO₂ and NO are 3 and 25 ppm, respectively [56].

According to the reaction scheme of the photo-oxidation of NO, the photocatalyst would be deactivated after long-term operation due to the coverage of active sites by adsorbed NO₃⁻ ions at the catalyst surface. However, the adsorbed NO₃⁻ ions could be easily washed away with 100 mL of D.I. water, enabling reuse of the catalyst. The removal rates of NO_x over 1st-, 2nd-, and 5th-reused TiO₂-Pt samples were indicated (Fig. 2A). The photocatalytic activity was only slightly decreased and becomes stable without significant reduction after two reaction–reuse cycles, in which over 96% of the photocatalytic activity remains functional (Fig. 2, 2nd, and 5th reused groups). The ICP-AES quantification further confirmed that the minor reduction of photocatalytic activity is due to the release of unstable Pt particles during reuses. The Pt content of the as-prepared/original TiO₂-Pt sample was 62 μmol/g TiO₂. While the Pt content in the 1st-, 2nd-, and 5th-rinsed water were 3.2, 0.2, and 0 (not detectable) μmol/g TiO₂-Pt, respectively. This suggests that most Pt particles on the TiO₂ surfaces are quite stable and thus TiO₂-Pt may be suitable for the development of additional antibacterial applications.

3.3. Bactericidal property of TiO₂-Pt photocatalysts

After physical characterizations, the bactericidal property of TiO₂-Pt against *S. aureus* was compared with other visible light-responsive photocatalysts (Fig. 3A, 48 mW/cm², 75 min). The ultraviolet (UV) light responsive photocatalysts ST01, P-25 and UV100 [34,39,40] were used as negative controls under visible light illumination (Fig. 3A). TiO₂-Pt samples were found to exhibit significantly higher bactericidal activity as compared with other tested samples including UV responsive photocatalysts ST01, P-25, UV100, visible-light responsive photocatalysts BA-PW25 (commercially available [37,38]), and C200 (a carbon-containing TiO₂ [23,34]) (Fig. 3A, ***, *P* < 0.001, vs. respective dark groups).

To obtain dose-dependent and kinetic data, we further analyzed the antibacterial activity against clinically isolated *S. aureus* at various intensities (28, 34 and 48 mW/cm², visible light) for 30 min (Fig. 3B) or fixed illumination density (48 mW/cm²) at various time intervals (0, 10, 15, 30, 45 and 75 min; Fig. 3C). Our results revealed that photocatalytic TiO₂-Pt substrates significantly reduced viable *S. aureus* cells within 30 min when exposed to visible light with doses higher than 34 mW/cm² (61.2 J/cm²; Fig. 3B). In addition, when the illumination density 48 mW/cm² was used, an efficient kill can be observed within 15 min (Fig. 3C, 15 min, TiO₂-Pt-light groups). Illumination of TiO₂-Pt by visible light significantly reduced the viable population of the bacteria (Fig. 3B and C; *, *P* < 0.05, **, *P* < 0.01, ***, *P* < 0.001, vs. respective untreated-dark groups).

To investigate the performance of TiO₂-Pt to eradicate other pathogenic bacteria, the antibacterial property against pathogenic *S. pyogenes* (toxin producing) and *A. baumannii* (nosocomial spreading)

was compared with *S. aureus* (48 mW/cm², 15 min; 43.2 J/cm²). Data revealed that the viable population of all tested pathogens was significantly reduced greater than 50% after the photocatalysis in this condition (Fig. 3D, *, *P* < 0.05, **, *P* < 0.01 and ***, *P* < 0.001, TiO₂-Pt, dark vs. light groups). In addition, *S. pyogenes* and *A. baumannii* are more sensitive to the photocatalysis than *S. aureus* (Fig. 3D, *S. pyogenes* and *A. baumannii* vs. *S. aureus*, TiO₂-Pt-light groups; *, *P* < 0.05, **, *P* < 0.01, ***, *P* < 0.001, vs. respective TiO₂-Pt-dark groups).

3.4. Photocatalysis reduced the survival rate of *S. aureus* after macrophage engulfment

Photocatalysis induces bacterial deformation [23], by which it reduced the resistance of phagocytic clearance, and contributed to the antibacterial effect of nitrogen-doped TiO₂ [28]. Thus, it was analyzed whether or not such antibacterial effect exists in this system (Suppl. Fig. S2). *S. aureus* was subjected to photocatalysis under a condition without significantly suppressing the viable bacteria (48 mW/cm², 5 min; Fig. 3C, no effect of TiO₂-Pt-light, 10 min groups). After a relatively short phagocytosis course (J774A.1 mouse macrophages [57]), we found that photocatalysis did not influence the phagocytic efficiency of photocatalyzed bacteria (Suppl. Fig. S2A, timetable; S2B, no significant differences among 0 h groups). However, the surviving bacteria significantly reduced in photocatalyzed groups after a longer engulfment and digestion by phagosomal enzymes (Suppl. Fig. S2B, TiO₂-Pt-light, 4 h groups vs. all other 4 h groups, **, *P* < 0.01). These results suggest that TiO₂-Pt-mediated photocatalysis likely induced temporal and recoverable bacterial damages, which could be recovered on the Luria-Bertani (LB) agar (Fig. 3C, no effect of TiO₂-Pt-light, 10 min),

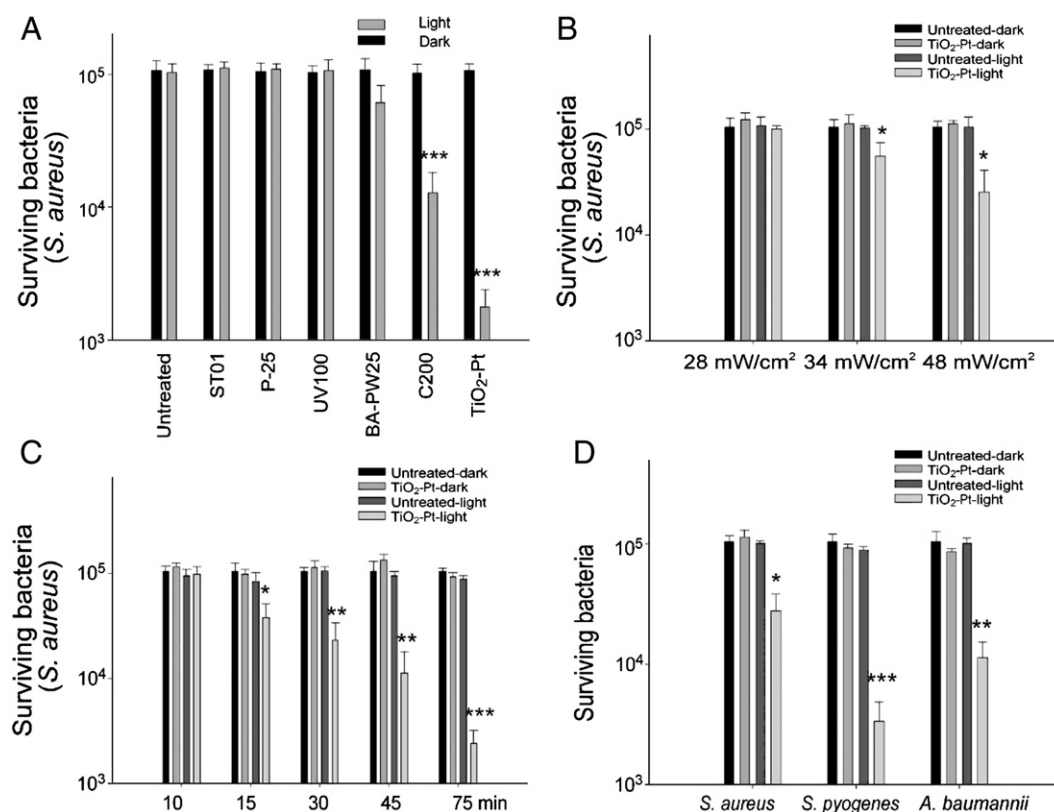


Fig. 3. Bactericidal property of TiO₂-Pt against *S. aureus*. Visible-light (48 mW/cm², 75 min, 337.5 J/cm²) induced bactericidal property of TiO₂-Pt was compared with UV-light responsive ST01, P-25, UV100, and UV/visible-light responsive BA-PW25, and C200 photocatalysts (A). ***, *P* < 0.001, vs. respective groups without illumination (dark groups). Untreated groups: without photocatalyst treatments. Dose dependent (B) and kinetic (C) analyses of the bactericidal activity of the TiO₂-Pt after visible light illumination are shown. Illumination was conducted either at different light densities (28, 34, 48 mW/cm²) for 30 min (50.4, 61.2 and 86.4 J/cm², respectively) (B) or at the same illumination density of 48 mW/cm² for different durations (10, 15, 30, 45, 75 min; 28.8, 43.2, 86.4, 129.6 and 337.5 J/cm², respectively) (C) on the elimination of *S. aureus* cells. (D) Visible-light (48 mW/cm², 15 min; 43.2 J/cm²) induced antibacterial activity of TiO₂-Pt against pathogenic bacteria including *S. aureus*, *S. pyogenes*, and *A. baumannii* was shown. The number of surviving bacteria (CFU) was indicated. **P* < 0.05, ***P* < 0.01 and ****P* < 0.001, compared to the respective TiO₂-Pt-dark groups. *n* = 6 (3 experiments with 2 replicates). The data are presented as mean ± SD.

but became extra-burdens for those phagocytosed bacteria to defend themselves against antibacterial mechanism of macrophages (Suppl. Fig. S2B, TiO₂-Pt light vs. dark, 4 h groups, **, $P < 0.01$). As damages of bacterial cells also contribute to the antibacterial outcome, killing efficiency may not fatefully reflect the overall antibacterial property of a photocatalyst. Accordingly, as compared with the traditional plating method, this phagocytosis assay is more realistic and sensitive to reveal relative attenuation levels of the bacteria.

3.5. Electron microscopic imaging of bacterial damages

To investigate the damages on photocatalyzed *S. aureus* cells, transmission electron microscopy (TEM) images of negative stained samples (Fig. 4A–F) and scanning electron microscopy (SEM) images were taken (Fig. 4G–H). When compared with the untreated (Fig. 4A–B) and non-photocatalyzed groups (Fig. 4E–G; in the dark), TiO₂-Pt-mediated photocatalysis (Fig. 4C–D, H) significantly induced damages on the bacteria. Photocatalysis causes perturbations on *S. aureus* cells (Fig. 4D, arrows), which are not observed in those bacteria without illumination (Fig. 4E–F). These results are in agreement with the SEM analysis, in which the deformation sites on the bacterial surfaces are revealed (Fig. 4H, white arrows, as compared with controls in the dark 5G).

3.6. Photocatalytic therapy mouse model

Aforementioned phagocytosis experiments indicated that TiO₂-Pt-mediated photocatalysis can attenuate bacteria *in vitro* (Suppl. Fig. S2). Accordingly, photocatalytic attenuation and elimination of pathogenic bacteria may be feasible *in vivo*. Before the *in vivo* experiments, we successfully analyzed the spectrum and demonstrated TiO₂-Pt-mediated antibacterial effect using mouse-skin penetrative visible-light (Suppl. Fig. S3). To further investigate the bactericidal property of TiO₂-Pt *in vivo*, an air-pouch infection mouse model was performed. Bacterial suspensions of *S. aureus* (3×10^5 CFU) were injected into the air pouches underneath the mouse skins and then illuminated the injection sites with skin-penetrative visible light using a cold-light source (KL-1500 LCD, 60 mW/cm²) for 30 min (Fig. 5A, experiment outline; Suppl. Fig. S4, experimental setting). Twenty-four hours later, the surviving bacteria (CFU) were then analyzed using the plating method. When compared with the control groups, both C200 (a carbon-containing TiO₂) [23] and TiO₂-Pt groups contained a reduced bacterial population after illumination (Fig. 5B, light vs. dark and untreated groups; *, $P < 0.05$, **, $P < 0.01$, vs. respective dark groups; †, $P < 0.05$, vs. C200 groups). In agreement with the *in vitro* analyses (Fig. 3A, Suppl. Fig. S3C), the bactericidal performance of TiO₂-Pt is significantly higher than C200 (Fig. 5, TiO₂-Pt vs. C200, light groups). These results suggest that TiO₂-Pt photocatalyst may have potentials to be developed as an antibacterial agent *in vivo*.

4. Discussion

Heavy traveling and urbanization enable infectious diseases to spread worldwide more rapidly. The emergence of virulent and antibiotic resistant pathogens leads to a requirement of alternative disinfection strategies in public environments [3–8]. Development of visible-light-responsive photocatalysts may be a feasible approach to against these pathogens. Classical photocatalysts are UV-responsive. To extend the light-absorption into visible-light range, TiO₂ composting with transition ions and/or anions is a common strategy to create intra-band gap states close to the conduction or valence band edges that cause visible-light absorption at the sub-band gap energies [26,29]. These materials are also able to inhibit the charge recombination in some conditions, thereby increase the photocatalytic activity [11,29]. As a result, the TiO₂-Pt photocatalyst was prepared in this study. Through NO-oxidation analysis, we confirmed that TiO₂-Pt has a higher visible-light inducible photocatalytic performance as compared with UV-

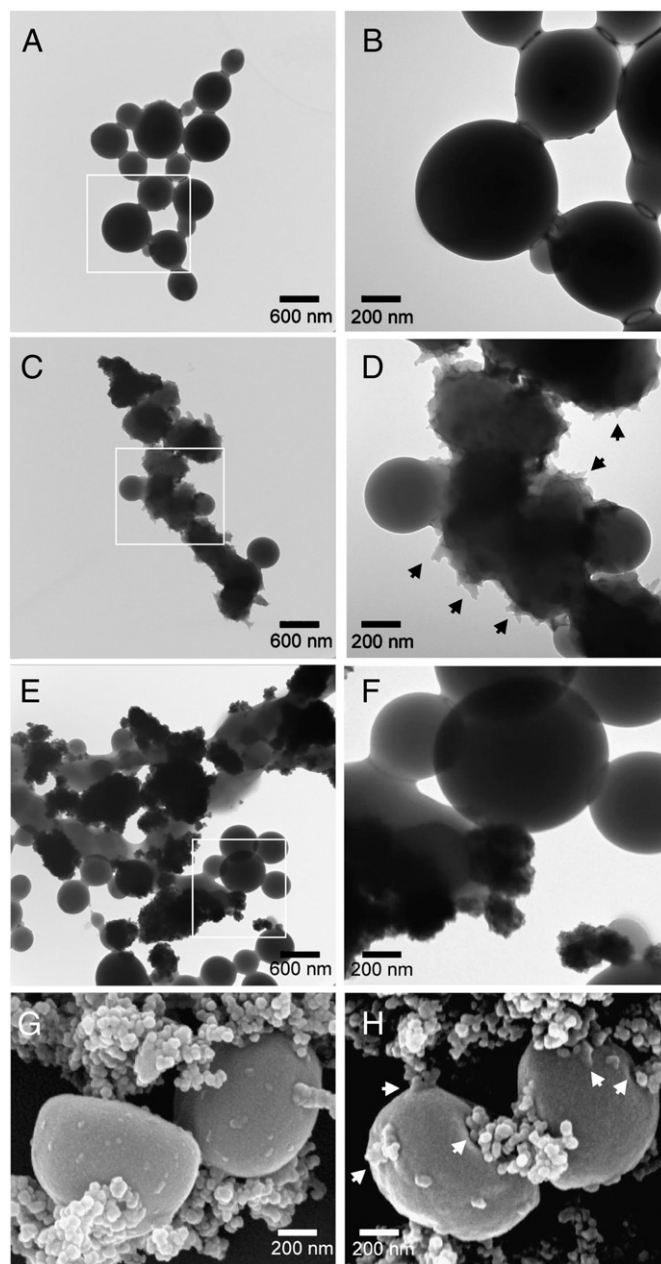


Fig. 4. Electron microscopy. Transmission electron microscopy (TEM) (A–F) and scanning electron microscopy (SEM) (G–H) images of *S. aureus* cells were taken before (A, B) and after TiO₂-Pt treatments (C–H), with (C, D, H) or without (E–G) illumination by visible light. A, C and E illustrate the low magnification images and B, D and F illustrate the high magnification images of TEM. G and H illustrate the high magnification images of SEM. The white squares highlighted in A, C and E represent the areas selected for B, D, and F, respectively. The arrows in D and H indicate the surface deformation sites of photocatalyzed bacteria. Scale bars: 600 nm in A, C and E, 200 nm in B, D, F–H. Representative images were selected from three independent experiments.

responsive (P25, UV100), and UV/visible-responsive (C200 and BA-PW25) TiO₂-based photocatalysts. In general, it has been reported that the TiO₂ photocatalytic reactions proceed mainly by the contributions of active oxygen species, such as hydroxyl radical, OH•, superoxide radical, O₂•⁻, and hydrogen peroxide, H₂O₂ [58–60]. Although these active species formation mechanisms have been suggested as photocatalytic oxidation and reduction of water and oxygen [58–60], the detailed mechanism on the TiO₂ surface is unclear so far, and a lot of efforts have been spent to elucidate the precise mechanism by many research groups [59,61,62]. It is hard to estimate the real quantum efficiency (Φ) of photocatalyst. Therefore, the apparent quantum efficiency

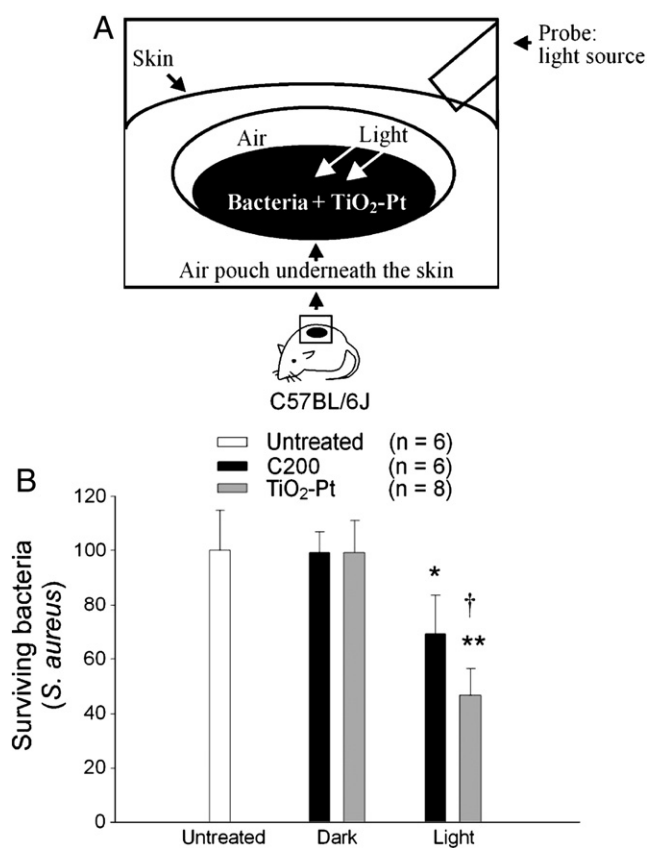


Fig. 5. TiO₂-Pt-mediated elimination of bacterial infection *in vivo*. Schematic illustration of the experiment is shown (A). After anesthesia and shaving the hairs of the injection site, mixtures of *S. aureus* (3×10^5 CFU) and photocatalyst nanoparticles (500 $\mu\text{g}/\text{mL}$, 0.3 mL PBS) were injected into air pouches of C57Bl/6J mice. The air pouches were then treated with (light) or without (dark) skin-penetrative visible light using a cold-light source (KL-1500 LCD, Carl Zeiss; 60 mW/cm^2) for 30 min (A). The quantitative results of the surviving bacteria are shown (CFU); the level of untreated groups (without photocatalysts and illumination) was normalized to 100% (B). * $P < 0.05$ and ** $P < 0.01$, compared to respective dark groups; † $P < 0.05$, vs. C200 groups. Untreated and C200 $n = 6$, TiO₂-Pt $n = 8$ (3 and 4 experiments with 2 replicates, respectively). The data are presented as mean \pm SD.

(Φ_{app}), amount of degraded compounds/amount of photo irradiated on photocatalyst, is usually used to show the activity of photocatalyst. The Φ_{app} for this work was further computed based on the following equation [56,63].

$$\varphi = \frac{(\text{mole of } (\text{NO} + \text{NO}_2) \text{ degraded})}{\text{Einstein of incident photons}}$$

The apparent quantum efficiencies for TiO₂-Pt, C200, BA-PW25, P25, UV100, and ST01 were 3.03, 1.88, 1.33, 0.41, 0.36, and 0.38%, which are consistent with the NO_x-removal activity. In agreement with the estimation on the apparent quantum efficiencies and the performance in NO-oxidation experiments (Fig. 2), TiO₂-Pt showed a superior bactericidal property after illuminated by visible light. Survival of human pathogens including *S. pyogenes*, *S. aureus* and *A. baumannii* is significantly suppressed (Fig. 3D).

Damages on bacterial cell wall/membrane are likely the key antibacterial step [64]. According to the TEM analysis, photocatalysis induced obvious damages on the bacterial surfaces (Fig. 4C–D). This is in part consistent with our experiments on *E. coli* cells, in which hole-like deformations were induced by photocatalysis [23]. Surviving bacteria after photocatalysis showed a reduced-resistance against

phagocytic clearance [28]. This suggests that such cellular damages and deformations may be an unaffordable burden when engulfed by a phagocyte. By contrast, these damages may be repairable if these bacteria were cultured in an optimal condition (e.g. on a dish with LB agar). In agreement with these observations, TiO₂-Pt photocatalyzed *S. aureus* cells showed a relatively lower resistance against phagocytosis in prolonged treatments (Suppl. Fig. S2B, TiO₂-Pt-light 4 h groups), indicating that TiO₂-Pt-mediated photocatalysis also induce such bacterial damages. Even though bacteria cannot be completely eliminated by photocatalysis, these results suggest that the remaining survivors are also greatly attenuated, and thus provide a promising approach for disinfection of pathogenic bacteria. In addition, these results suggest that TiO₂-Pt-mediated attenuation of bacteria could be feasible *in vivo*.

Even though antibacterial effect of TiO₂ photocatalysts has been well-documented in thin film and polymer composites [12–21,27,28,32], the use of nanoparticles is a relatively feasible approach to be applied *in vivo*. In the animal experiments, TiO₂-Pt nanoparticle-mediated bacterial killing was successfully demonstrated in mice. We found that TiO₂-Pt more efficiently eliminated pathogenic bacteria than another visible light responsive photocatalyst C200 in an air pouch model. Despite these results, evidences have implied that exposure to TiO₂ can cause side effects such as procoagulant and inflammatory responses [65–67]. Activation of platelets and coagulant factors by TiO₂ surfaces can lead to procoagulant activation and thus limit dental applications that make contact with patient tissue [65–67]. Through measuring the blood counts and a marker of liver-function aspartate aminotransferase (AST), here we found that the TiO₂-Pt treatments did not induce significant pathogenic side effects in mice (Suppl. Fig. S5). Unlike commercially available BA-PW25 and carbon-containing TiO₂ C200, TiO₂-Pt injections did not elicit side effects such as thrombocytopenia and liver damage (Suppl. Fig. S5; these two phenotypes implicate the platelet activation, procoagulant and inflammatory responses [46,65,66,68,69]). This suggested that TiO₂-Pt is more suitable for *in vivo* usages as compared with other materials tested in this study. Literatures have indicated that adverse effects such as cyto- and geno-toxic effects of nanomaterials are primarily caused by the induction of oxidative stress [70,71]. Since oxidative stress can induce inflammation and liver damages [72], the different behavior of TiO₂-Pt versus BA-PW25 and C200 *in vivo* may be resulted by similar mechanism. A detailed molecular pathway that leads to different responses *in vivo* after various TiO₂ photocatalysts treatments is an interesting issue and worthy to be further investigated.

Although the antibacterial performance of visible-light activated TiO₂-Pt may not match with conventional disinfectants such as alcohols, iodine and chlorine, these disinfectants are not suitable for *in vivo* applications. As the antibacterial mechanism is different from the antibiotics, photocatalysts have potentials to be developed as an alternative approach to eliminate drug-resistant bacteria. In addition, compared to carbon and silver containing TiO₂, on which the carbon is gradually decomposed and the silver is continuously releasing into the rinsed water that leads to a reduction of visible-light stimulated photocatalytic performance (authors' unpublished results), TiO₂-Pt is highly stable after various reuses. Furthermore, under visible light stimulation, TiO₂-Pt exerts superior quantum efficiency and better bactericidal photocatalytic performance on the elimination of pathogenic bacteria when compared to several commercially available and laboratory-prepared UV/visible-responsive photocatalysts (UV-responsive: ST01, P25, UV100, and visible-responsive: C200, BA-PW25). At the same time, TiO₂-Pt-mediated photocatalysis is able to eliminate subcutaneously infected bacteria. In addition to the killing, the bacterial damages induced prior to the exposure to host defense system also facilitated the phagocytic clearance. Thus, these findings suggest that the visible-light responsive TiO₂-Pt photocatalyst have potential applications on the development of a highly effective antibacterial material in both *in vitro* and *in vivo* settings.

Acknowledgements

The authors wish to thank the assistances from the Electron Microscopy Laboratory of Tzu Chi University. This work was supported by National Science Council of Taiwan, Republic of China, under grant no. NSC 95-2311-B-320-006, 95-2811-B-320-001, 96-2311-B-320-005-MY3, 98-2320-B-320-004-MY3, and 99-2311-B-320-003-MY3; and Tzu-Chi University under grant no. TCIRP 95002-02, TCIRP 96004-01, TCIRP 98001-01, TCRPP 99020-01 and TCRPP100003.

Appendix A. Supplementary data

Supplementary data to this article can be found online at <http://dx.doi.org/10.1016/j.bbagen.2013.03.022>.

References

- [1] G. McDonnell, A.D. Russell, Antiseptics and disinfectants: activity, action, and resistance, *Clin. Microbiol. Rev.* 12 (1999) 147–179.
- [2] A.D. Russell, Biocide use and antibiotic resistance: the relevance of laboratory findings to clinical and environmental situations, *Lancet Infect. Dis.* 3 (2003) 794–803.
- [3] A.E. Aiello, E. Larson, Antibacterial cleaning and hygiene products as an emerging risk factor for antibiotic resistance in the community, *Lancet Infect. Dis.* 3 (2003) 501–506.
- [4] E.Y. Furuya, F.D. Lowy, Antimicrobial-resistant bacteria in the community setting, *Nat. Rev. Microbiol.* 4 (2006) 36–45.
- [5] A.D. Russell, Bacterial adaptation and resistance to antiseptics, disinfectants and preservatives is not a new phenomenon, *J. Hosp. Infect.* 57 (2004) 97–104.
- [6] G. Taubes, The bacteria fight back, *Science* 321 (2008) 356–361.
- [7] M.W. Wassenberg, G.A. de Wit, B.A. van Hout, M.J. Bonten, Quantifying cost-effectiveness of controlling nosocomial spread of antibiotic-resistant bacteria: the case of MRSA, *PLoS One* 5 (2010) e11562.
- [8] C.A. Arias, B.E. Murray, Antibiotic-resistant bugs in the 21st century—a clinical super-challenge, *N. Engl. J. Med.* 360 (2009) 439–443.
- [9] A. Fujishima, K. Honda, Electrochemical photolysis of water at a semiconductor electrode, *Nature* 238 (1972) 37–38.
- [10] Q. Li, S. Mahendra, D.Y. Lyon, L. Brunet, M.V. Liga, D. Li, P.J. Alvarez, Antimicrobial nanomaterials for water disinfection and microbial control: potential applications and implications, *Water Res.* 42 (2008) 4591–4602.
- [11] K. Hashimoto, H. Irie, A. Fujishima, TiO₂ photocatalysis: a historical overview and future prospects, *Jpn. J. Appl. Phys.* 44 (2005) 8269–8285.
- [12] O. Akhavan, R. Azimirad, S. Safa, M.M. Larjani, Visible light photo-induced antibacterial activity of CNT-doped TiO₂ thin films with various CNT contents, *J. Mater. Chem.* 20 (2010) 7386–7392.
- [13] G. Jiang, J. Zeng, Preparation of nano-TiO₂/polystyrene hybride microspheres and their antibacterial properties, *J. Appl. Polym. Sci.* 116 (2010) 779–784.
- [14] H.R. Pant, D.R. Pandeya, K.T. Nam, W.I. Baek, S.T. Hong, H.Y. Kim, Photocatalytic and antibacterial properties of a TiO₂/nylon-6 electrospun nanocomposite mat containing silver nanoparticles, *J. Hazard. Mater.* 189 (2011) 465–471.
- [15] R.A. Damodar, S.J. You, H.H. Chou, Study the self cleaning, antibacterial and photocatalytic properties of TiO₂ entrapped PVDF membranes, *J. Hazard. Mater.* 172 (2009) 1321–1328.
- [16] W. Su, S. Wang, X. Wang, X. Fu, J. Weng, Plasma pre-treatment and TiO₂ coating of PMMA for the improvement of antibacterial properties, *Surf. Coat. Technol.* 205 (2010) 465–469.
- [17] H. Kong, J. Song, A. Jang, Photocatalytic antibacterial capabilities of TiO₂-biocidal polymer nanocomposites synthesized by a surface-initiated photopolymerization, *Environ. Sci. Technol.* 44 (2010) 5672–5676.
- [18] X. Sang, P. Wang, L. Ai, Y. Li, J. Bu, Preparation and characterization of nano-TiO₂/PE antibacterial films, *Adv. Mater. Res.* 284–286 (2011) 1790–1793.
- [19] O. Akhavan, Lasting antibacterial activities of Ag-TiO₂/Ag-a-TiO₂ nanocomposite thin film photocatalysts under solar light irradiation, *J. Colloid Interface Sci.* 336 (2009) 117–124.
- [20] O. Akhavan, E. Ghaderi, Photocatalytic reduction of graphene oxide nanosheets on TiO₂ thin film for photoinactivation of bacteria in solar light irradiation, *J. Phys. Chem. C* 113 (2009) 20214–20220.
- [21] O. Akhavan, M. Abdolohad, Y. Abdi, S. Mohajerzadeh, Synthesis of titania/carbon nanotube heterojunction arrays for photoinactivation of *E. coli* in visible light irradiation, *Carbon* 47 (2009) 3280–3287.
- [22] J.W. Liou, H.H. Chang, Bactericidal effects and mechanisms of visible light-responsive titanium dioxide photocatalysts on pathogenic bacteria, *Arch. Immunol. Ther. Exp.* 60 (2012) 267–275.
- [23] J.W. Liou, M.H. Gu, Y.K. Chen, W.Y. Chen, Y.C. Chen, Y.H. Tseng, Y.J. Hung, H.H. Chang, Visible light responsive photocatalyst induces progressive and apical-terminus preferential damages on *Escherichia coli* surfaces, *PLoS One* 6 (2011) e19982.
- [24] R.P. Gallagher, T.K. Lee, Adverse effects of ultraviolet radiation: a brief review, *Prog. Biophys. Mol. Biol.* 92 (2006) 119–131.
- [25] M. Iwasaki, M. Hara, H. Kawada, H. Tada, S. Ito, Cobalt ion-doped TiO₂ photocatalyst response to visible light, *J. Colloid Interface Sci.* 224 (2000) 202–204.
- [26] R. Asahi, T. Morikawa, T. Ohwaki, K. Aoki, Y. Taga, Visible-light photocatalysis in nitrogen-doped titanium oxides, *Science* 293 (2001) 269–271.
- [27] M.S. Wong, W.C. Chu, D.S. Sun, H.S. Huang, J.H. Chen, P.J. Tsai, N.T. Lin, M.S. Yu, S.F. Hsu, S.L. Wang, H.H. Chang, Visible-light-induced bactericidal activity of a nitrogen-doped titanium photocatalyst against human pathogens, *Appl. Environ. Microbiol.* 72 (2006) 6111–6116.
- [28] J.H. Kau, D.S. Sun, H.H. Huang, M.S. Wong, H.C. Lin, H.H. Chang, Role of visible light-activated photocatalyst on the reduction of anthrax spore-induced mortality in mice, *PLoS One* 4 (2009) e4167.
- [29] H. Kisch, W. Macyk, Visible-light photocatalysis by modified titania, *Chemphyschem* 3 (2002) 399–400.
- [30] W. Macyk, H. Kisch, Photosensitization of crystalline and amorphous titanium dioxide by platinum (IV) chloride surface complexes, *Chem. Eur. J.* 7 (2001) 1862–1867.
- [31] A.D. Russell, W.B. Hugo, Antimicrobial activity and action of silver, *Prog. Med. Chem.* 31 (1994) 351–370.
- [32] M.S. Wong, D.S. Sun, H.H. Chang, Bactericidal performance of visible-light responsive titania photocatalyst with silver nanostructures, *PLoS One* 5 (2010) e10394.
- [33] B. Tryba, Increase of the photocatalytic activity of TiO₂ by carbon and iron modifications, *Int. J. Photoenergy* 2008 (2008) 1–15.
- [34] C.L. Cheng, D.S. Sun, W.C. Chu, Y.H. Tseng, H.C. Ho, J.B. Wang, P.H. Chung, J.H. Chen, P.J. Tsai, N.T. Lin, M.S. Yu, H.H. Chang, The effects of the bacterial interaction with visible-light responsive titania photocatalyst on the bactericidal performance, *J. Biomed. Sci.* 16 (2009) 7.
- [35] T. Matsunaga, R. Tomoda, T. Nakajima, H. Wake, Photoelectrochemical sterilization of microbial cells by semiconductor powders, *FEMS Microbiol. Lett.* 29 (1985) 211–214.
- [36] Y.L. Chen, Y.S. Chen, H. Chan, Y.H. Tseng, S.R. Yang, H.Y. Tsai, H.Y. Liu, D.S. Sun, H.H. Chang, The use of nanoscale visible light-responsive photocatalyst TiO₂-Pt for the elimination of soil-borne pathogens, *PLoS One* 7 (2012) e31212.
- [37] S. Matsuzawa, C. Maneerat, Y. Hayata, T. Hirakawa, N. Negishi, T. Sano, Immobilization of TiO₂ nanoparticles on polymeric substrates by using electrostatic interaction in the aqueous phase, *Appl. Catal. Environ.* 83 (2008) 39–45.
- [38] T. Sano, E. Puzenat, C. Guillard, C. Geantet, S. Matsuzawa, Degradation of C₂H₂ with modified-TiO₂ photocatalysts under visible light irradiation, *J. Mol. Catal. A Chem.* 284 (2008) 127–133.
- [39] Y.M. Lin, Y.H. Tseng, J.H. Huang, C.C. Chao, C.C. Chen, I. Wang, Photocatalytic activity for degradation of nitrogen oxides over visible light responsive titania-based photocatalysts, *Environ. Sci. Technol.* 40 (2006) 1616–1621.
- [40] T.M. Tsai, H.H. Chang, K.C. Chang, L.Y. Liu, C.C. Tseng, A comparative study of the bactericidal effect of photocatalytic oxidation by TiO₂ on antibiotic-resistant and antibiotic-sensitive bacteria, *J. Chem. Technol. Biotechnol.* 85 (2010) 1642–1653.
- [41] N. Negishi, K. Takeuchi, T. Ibusuki, The surface structure of titanium dioxide thin film photocatalyst, *Appl. Surf. Sci.* 121 (1997) 417–420.
- [42] Y.H. Tseng, C.H. Kuo, Photocatalytic degradation of dye and NO_x using visible-light-responsive carbon-contained TiO₂, *Catal. Today* 174 (2011) 114–120.
- [43] Y.H. Tseng, C.S. Kuo, C.H. Huang, Y.Y. Li, P.W. Chou, C.L. Cheng, M.S. Wong, Visible-light-responsive nano-TiO₂ with mixed crystal lattice and its photocatalytic activity, *Nanotechnology* 17 (2006) 2490–2497.
- [44] I. 22197-1, Fine Ceramics (Advanced Ceramics, Advanced Technical Ceramics) – Test Method for Air-purification Performance of Semiconducting Photocatalytic Materials – Part 1: Removal of Nitric Oxide, International Organization for Standardization (ISO), 2007.
- [45] W.K. Chang, D.S. Sun, H. Chan, P.T. Huang, W.S. Wu, C.H. Lin, Y.H. Tseng, Y.H. Cheng, C.C. Tseng, H.H. Chang, Visible light responsive core-shell structured In₂O₃@CaIn₂O₆ photocatalyst with superior bactericidal property and biocompatibility, *Nanomedicine* 8 (2012) 609–617.
- [46] H.S. Huang, D.S. Sun, T.S. Lien, H.H. Chang, Dendritic cells modulate platelet activity in IVlg-mediated amelioration of ITP in mice, *Blood* 116 (2010) 5002–5009.
- [47] O. Akhavan, E. Ghaderi, Self-accumulated Ag nanoparticles on mesoporous TiO₂ thin film with high bactericidal activities, *Surf. Coat. Technol.* 204 (2010) 3676–3683.
- [48] Y.-L. Kuo, H.-W. Chen, Y. Ku, Analysis of silver particles incorporated on TiO₂ coatings for the photodecomposition of o-cresol, *Thin Solid Films* 515 (2007) 3461–3468.
- [49] Y.-H. Tseng, B.-K. Huang, Photocatalytic degradation of NO_x using Ni-containing TiO₂, *Int. J. Photoenergy* 2012 (2012) 1–7.
- [50] F. Zhang, J. Chen, X. Zhang, W. Gao, R. Jin, N. Guan, Y. Li, Synthesis of titania-supported platinum catalyst: the effect of pH on morphology control and valence state during photodeposition, *Langmuir* 20 (2004) 9329–9334.
- [51] Y.-H. Tseng, H.-Y. Lin, C.-S. Kuo, Y.-Y. Li, C.-P. Huang, Thermostability of nano-TiO₂ and its photocatalytic activity, *React. Kinet. Catal. Lett.* 89 (2006) 63–69.
- [52] B.D. Cullity, S.R. Stock, Elements of X-ray Diffraction, 3rd ed., Prentice-Hall Inc., 2001.
- [53] F.J. Kelly, G.W. Fuller, H.A. Walton, J.C. Fussell, Monitoring air pollution: use of early warning systems for public health, *Respirology* 17 (2012) 7–19.
- [54] R. Atkinson, D.L. Baulch, R.A. Cox, J.R.F. Hampson, J.A. Kerr, J. Troe, Evaluated kinetic and photochemical data for atmospheric chemistry: supplement III, *J. Phys. Chem. Ref. Data* 18 (1989) 881–1097.
- [55] S.Y. Treschev, P.W. Chou, Y.H. Tseng, J.B. Wang, E.V. Perevedentseva, C.L. Cheng, Photoactivities of the visible-light-activated mixed-phase carbon-containing titanium dioxide: the effect of carbon incorporation, *Appl. Catal. Environ.* 79 (2007) 8–16.
- [56] Y.H. Tseng, C.S. Kuo, C.H. Huang, Y.Y. Li, Preparation of visible-light-responsive nitrogen-carbon co-doped titania by chemical vapor deposition, *Z. Phys. Chem.* 224 (2010) 843–856.
- [57] J.H. Kau, D.S. Sun, H.S. Huang, T.S. Lien, H.H. Huang, H.C. Lin, H.H. Chang, Sublethal doses of anthrax lethal toxin on the suppression of macrophage phagocytosis, *PLoS One* 5 (2010) e14289.
- [58] V. Brezova, A. Stasko, Spin trap study of hydroxyl radicals formed in the photocatalytic system TiO₂-water-p-cresol-oxygen, *J. Catal.* 147 (1994) 156–162.

- [59] T. Hirakawa, K. Yawata, Y. Nosaka, Photocatalytic reactivity for $O_2^{\bullet-}$ and OH^- radical formation in anatase and rutile TiO_2 suspension as the effect of H_2O_2 addition, *Appl. Catal. A* 325 (2007) 105–111.
- [60] Y. Nosaka, M. Kishimoto, J. Nishino, Factors governing the initial process of TiO_2 photocatalysis studied by means of in-situ electron spin resonance measurements, *J. Phys. Chem. B* 102 (1998) 10279–10283.
- [61] K. Ishibashi, A. Fujishima, T. Watanabe, K. Hashimoto, Quantum yields of active oxidative species formed on TiO_2 photocatalyst, *J. Photochem. Photobiol. A* 134 (2000) 139–142.
- [62] R. Nakamura, Y. Nakato, Primary intermediates of oxygen photoevolution reaction on TiO_2 (rutile) particles, revealed by in situ FTIR absorption and photoluminescence measurements, *J. Am. Chem. Soc.* 126 (2004) 1290–1298.
- [63] Test Method for Air-purification Performance of Semiconducting Photocatalytic Materials – Part 1: Removal of Nitric Oxide, ISO, 2003. , (22197-22191:22007).
- [64] P.C. Maness, S. Smolinski, D.M. Blake, Z. Huang, E.J. Wolfrum, W.A. Jacoby, Bactericidal activity of photocatalytic TiO_2 reaction: toward an understanding of its killing mechanism, *Appl. Environ. Microbiol.* 65 (1999) 4094–4098.
- [65] M.F. Maitz, M.T. Pham, E. Wieser, I. Tsyganov, Blood compatibility of titanium oxides with various crystal structure and element doping, *J. Biomater. Appl.* 17 (2003) 303–319.
- [66] A. Nemmar, K. Melghit, B.H. Ali, The acute proinflammatory and prothrombotic effects of pulmonary exposure to rutile TiO_2 nanorods in rats, *Exp. Biol. Med.* (Maywood) 233 (2008) 610–619.
- [67] A. Thor, L. Rasmusson, A. Wennerberg, P. Thomsen, J.M. Hirsch, B. Nilsson, J. Hong, The role of whole blood in thrombin generation in contact with various titanium surfaces, *Biomaterials* 28 (2007) 966–974.
- [68] D.S. Sun, C.C. King, H.S. Huang, Y.L. Shih, C.C. Lee, W.J. Tsai, C.C. Yu, H.H. Chang, Antiplatelet autoantibodies elicited by dengue virus non-structural protein 1 cause thrombocytopenia and mortality in mice, *J. Thromb. Haemost.* 5 (2007) 2291–2299.
- [69] Y. Cui, H. Liu, M. Zhou, Y. Duan, N. Li, X. Gong, R. Hu, M. Hong, F. Hong, Signaling pathway of inflammatory responses in the mouse liver caused by TiO_2 nanoparticles, *J. Biomed. Mater. Res. A* 96 (2011) 221–229.
- [70] A. Nel, T. Xia, L. Madler, N. Li, Toxic potential of materials at the nanolevel, *Science* 311 (2006) 622–627.
- [71] A.A. Shvedova, V.E. Kagan, B. Fadeel, Close encounters of the small kind: adverse effects of man-made materials interfacing with the nano-cosmos of biological systems, *Annu. Rev. Pharmacol. Toxicol.* 50 (2010) 63–88.
- [72] Y.J. Kim, E.H. Kim, K.B. Hahm, Oxidative stress in inflammation-based gastrointestinal tract diseases: challenges and opportunities, *J. Gastroenterol. Hepatol.* 27 (2012) 1004–1010.